J|A|C|S
ARTICLES
Published on Web 10/23/2004

Selective Dispersion of Single-Walled Carbon Nanotubes in the Presence of Polymers: the Role of Molecular and Colloidal Length Scales

Rina Shvartzman-Cohen,[†] Einat Nativ-Roth,[†] Ezhil Baskaran,[‡] Yael Levi-Kalisman,[§] Igal Szleifer,*[,‡] and Rachel Yerushalmi-Rozen*[,†,§]

Contribution from the Department of Chemical Engineering, Ben Gurion University in the Negev, 84105 Beer Sheva, Israel; Department of Chemistry, Purdue University, 560 Oval Drive, West Lafayette, Indiana 47907; The Ilse Katz Center for Meso- and Nanoscale Science and Technology, Ben Gurion University in the Negev, 84105 Beer Sheva, Israel

Received June 19, 2004; E-mail: rachely@bgumail.bgu.ac.il; igal@purdue.edu

Abstract: Dimensionality is known to play a key role in the solution behavior of nano- and mesoparticles. In particular, the shape and the range of the attractive van der Waals interparticle potential are determined by the number of microscopic versus mesoscopic dimensions. For single-walled nanotubes (SWNTs), where two of the dimensions are nanoscopic and one is mesoscopic, the intertube attraction is relatively short ranged, albeit very steep. The very large attraction (compared to the thermal energy, K_bT) among long SWNTs leads to aggregation at different levels and constitutes a major barrier for manipulation and utilization of SWNTs. This study demonstrates that it is possible to shape the intertube potential by decorating SWNTs with end-tethered polymers. In good solvent conditions for the polymers, entropic repulsion among the tethered chains generates a free energy barrier that prevents SWNTs from approaching the attractive part of the intertube potential. Consequentially, stable dispersions of individual, well separated SWNTs can be prepared. Investigation of different chain lengths and tethering densities of the polymers as well as the interparticle potentials for nanometric versus mesoscopic particles suggests that polymer-induced steric stabilization provides a generic method for separation of SWNTs from mixtures of colloidal species, as demonstrated experimentally.

Introduction

Stabilization of colloidal dispersions is an old technological problem first attempted in ancient China and Egypt[1] where a natural polysaccharide, Gum Arabic (GA), was used in the preparation of carbon-black ink. Indeed, ink is an example for a typical colloidal system where solid spherical particles are dispersed in a liquid via the adsorption of a polymer. Such dispersions are considered to be stable as long as the individual particles do not aggregate or coagulate, and the approach is known as *steric stabilization.*[2] While the utilization of polymers for stabilization of colloidal dispersions is a few thousands years old, thorough understanding of polymer−colloid interactions has emerged only over the last 30 years or so. An even younger field is that of interactions among polymers and pseudo-one-dimensional nanocolloids, known as single-walled carbon nanotubes (SWNTs).[3] Over the past few years polymers have been utilized for noncovalent dispersing of SWNTs in different media. Yet, an understanding of SWNT−polymers interactions is only beginning to emerge. In the following we present the relevant terms, suggest a model that accounts for the generic nature of polymer−SWNT interactions, predict that the interactions may lead to dimensional selectivity that may be utilized for purification of SWNT, and demonstrate the concept.

Background. A key term in colloidal interactions is the interparticle potential.[4] For noncharged, spherical particles of radii a, it is common to assume that the van der Waals (vdW) interactions are nonretarded[4] and additive. The resulting vdW potential between the particles, $V(r)$, where r is the interparticle distance is described by $V(r) = -A_{\text{eff}}/12a/r$ for $r \ll a$, $V(r) \propto A_{\text{eff}}a/r^6$ for $r \gg a$ and a more complicated expression in the intermediate range.[5] For all separations, r, the interparticle potential is proportional to the particle size, a. The other proportionality constant is A_{ij}, the effective Hamaker constant which depends on the nature of the particles and the intervening liquid.[6] For typical particles, with a radius in the order of a few hundred nanometers, the attractive interaction exceeds the thermal energy at separations larger than the particle radius.

[†] Department of Chemical Engineering, Ben Gurion University in the Negev.
[‡] Purdue University.
[§] The *Ilse Katz* Center for Meso- and Nanoscale Science and Technology, Ben Gurion University in the Negev.

(1) *Encyclopedia Britannica* 257−259; William Benton: Chicago, 1966.
(2) Napper, D. H., Ed.; *Polymeric Stabilization of Colloidal Dispersions;* Academic Press, Inc.: Orlando, FL, 1993.
(3) Dresselhaus, M. S.; Dresselhaus, G.; Avouris, Ph., Eds. *Carbon Nanotubes, Topics in Applied Physics* 80; Springer-Verlag: Berlin, Heidelberg, 2001.
(4) Israelachvili, J., Ed. *Intermolecular and Surface Forces*; Academic Press Inc.: San Diego, 1992.
(5) The nonretarded vdW interaction free energy (W) between two mesoscopic cylinders is $W = AL/12\sqrt{2}D^{3/2}(R_1R_2/R_1 + R_2)^{1/2}$ where A is the Hamaker constant, L, the cylinder length, D, the intercylinder distance, and R_1, R_2 the radius of each of the cylinders. Chapter 11, ref 4.

10.1021/ja046377c CCC: $27.50

Thus, long term stability (of either kinetic or thermodynamic origin) can only be imparted by the prevalence of a repulsion of sufficient range and magnitude, such as the long ranged osmotic (steric) repulsion among tethered polymers in good solvent conditions. Among the more efficient steric stabilizers are block-copolymers.[7] Block copolymers are comprised of covalently bonded chemically distinct and often mutually incompatible moieties (designated A−B and A−B−A for diblocks and triblocks, respectively). A typical scenario for steric stabilization via block copolymers relies on the dual action of the polymer due to a selective interaction with the solvent: while one of the blocks (A) anchors the chain to the surface, the other block (B) dangles into the solvent and repels other polymers. It is well-known that with this type of anchoring the density and the molecular weight of the tethered chains dominate the details of the modified interparticle potential.[8,9]

In addition, the properties of colloidal dispersions are affected by the size, shape, and dimensions of the dispersed particles, as these parameters strongly modify the interparticle potential. When dealing with nonspherical particles, such as platelike clays or submicron rods, it is common to assume that their qualitative behavior is well represented in terms of an equivalent sphere, or to account for the geometry.[2] However, these assumptions should be examined carefully when two of the dimensions are nanometric, as is the case for SWNTs.

SWNTs are crystalline graphitic rods, characterized by a diameter in the range 1−2 nm and a typical length of microns[10] resulting in an aspect ratio larger than 1000. Pristine SWNT form vdW crystals, known as "ropes" or "bundles" of typically 100−500 tubes.[3] Bundling was found to act as an obstacle to most applications and results in diminished mechanical and electrical properties as compared to theoretical predictions related to individual SWNT.[11]

A large effort has been invested during the past decade in the development of approaches for dispersing individual SWNT in aqueous and organic media.[12−16] A variety of methods were designed to induce short ranged repulsion among the tubes: these include covalent modifications,[12,13] $\pi-\pi$ interactions,[14,15] surfactant adsorption,[16] and more.[17] Consequentially these treatments were often found to result in modification of the structural, electronic, and mechanical properties of the tubes[18−20]

Due to the shortcomings of these approaches, noncovalent methods mainly based on physical adsorption of polymers were developed. [21−23] While quite a few examples were reported, the underlying mechanism in each of these studies was believed to rely on specific interactions between a given polymer and the SWNTs. For example, it was suggested that tight SWNT−polymer association (known as "wrapping") leads to screening of the hydrophobic interaction in aqueous solutions and consequential dispersion of tubes.[21]

Recently, we presented a generic approach for stabilization of SWNT dispersions in aqueous and organic liquids, using synthetic and natural block copolymers.[24,25] We showed that a large variety of di- and triblock copolymers in selective solvent (aqueous as well as organic) conditions are efficient stabilizers. Following a temporary exfoliation and deagglomeration of SWNT (for example, via gentle sonication)[26] adsorption of block copolymers prevents reaggregation. This observation is somewhat surprising, as the adhesion energy at the minimum of the intertube potential is known to exceed a few thousands of K_bT[27] by far prevailing entropic (steric) repulsion among polymeric chains.

Here we investigate the origins of the observed behavior by determining the intertube potential for SWNTs decorated by end-tethered polymers. For the attractive part we use the intertube potential calculated by Girifalco et. al..[27] For the repulsive part we generalize a molecular theory that explicitly accounts for the conformational degrees of freedom of the polymer chains.[28,29] The results suggest that, due to the steepness and short-ranged nature of the potential, a relatively weak repulsion, such as the osmotic repulsion among tails of tethered copolymers in a good solvent for the tail chains, can stabilize the dispersed SWNTs and prevent SWNTs from approaching the attractive minimum.

Following the theoretical calculations we suggest that polymer−colloid interactions are sensitive to the dimensions of the dispersed particles and the length of the polymeric chains. We demonstrate (experimentally) that polymers, which disperse SWNT, may not disperse fullerens, carbon fibers, and graphite flakes and that this inherent selectivity can be used for purification of SWNT−particle mixtures.

Experimental Section

Materials: Raw SWNTs from three different sources were used in this study. SWNTAP was purchased from Carbolex Inc. USA (SWNTAP http://carbolex.com), SWNTRW was purchased from

(6) Note that the effective Hamaker constant $A_{ij} = \pi^2\alpha_{ij}n_in_j$, where α_{ji} is the effective polarizability, $\alpha_{ij} = (\alpha_{ii}\alpha_{jj})^{1/2}$, and n_i and n_j are the number density of species i and j correspondingly. $A_{eff} = A_{LS} - A_{LL}$, where L represents the liquid, and S, the solid colloidal particles.

(7) Hadjichristidis, N.; Pispas, S.; Floudas, G. *Block Copolymers: Synthetic Strategies, Physical Properties, and Applications*; John Wiley & Sons: Europe, 2003.
(8) Taunton, H. J.; Toprakciaglu, C.; Fetters, L. J; Klein, J. *Macromolecules* **1990**, *23*, 571.
(9) Halperin, A.; Tirrell, M.; Lodge, T. P. *Adv. Polym. Sci*. **1999**, *100*, 39.
(10) Recently SWNTs of a few centimeters were reported: Zhu, H. W.; Xu, C. L.; Wu, D. H.; Wei, B. Q.; Vajtai, R.; Ajayan, P. M. *Science* **2002**, *296*, 884−886.
(11) Baughman, R. H.; Zakhidov, A. A.; de Heer, W. A. *Science* **2002**, *297*, 787.
(12) Chen, J.; Hamon, M. A.; Hu, H; Chen, Y.; Rao, A. M.; Eklund, P. C.; Haddon, R. C. *Science* **1998**, *282*, 95−98.
(13) Ausman, K. D.; Piner, R.; Lourie, O.; Ruoff, R. S.; Korobov, M. *J. Phys. Chem. B* **2000**, *104*, 8911−8915.
(14) Coleman, J. N.; Dalton, A. B.; Curran, S.; Rubio, A.; Barklie, R. C.; Blau, W. J. *Adv. Mater*. **2000**, *12*, 213−216.
(15) Shin, M.; Wong, N.; Shi Kam, Chen, R. J.; Li, Y.; Dai, H. *Nano Lett.* **2000**, *2*, 285−288.
(16) Vigolo, B.; Penicaud, A.; Coulon, C.; Sauder, R.; Pailler, C.; Journet, P.; Bernier, P.; Poulin, P. *Science* **2000**, *290*, 1331−1334.
(17) Zheng, M.; Jagota, A.; Strano, M. S.; Santos, A. P.; Barone, P.; Chou, S. G.; Diner, B. A.; Dresselhaus, M. S.; McLean, R. C.; Onoa, G. B.; Samsonidze, G. G.; Semke, E. D.; Usrey, M.; Walls, D. J. *Science* **2003**, *302*, 1545−48.
(18) Monthioux, M.; Smith, B. W.; Claye, A.; Fischer, J. E.; Luzzi, D. E. *Carbon* **2001**, *39*, 1251.
(19) Garg, A.; Sinnott, S. B. *Chem. Phys. Lett*. **1998**, *295*, 273−278.
(20) Chen, J.; Liu, H.; Weimer, W. A.; Halls, M. D.; Waldeck, D. H.; Walker, G. C. *J. Am. Chem. Soc*. **2002**, *124*, 9034.
(21) O'Connell, M. J.; Boul, P. J.; Ericson, L. M.; Huffman, C.; Wang, Y. H.; Haroz, E. H.; Kuper, C.; Tour, J.; Ausman, K. D.; Smalley, R. E. *Chem. Phys. Lett.* **2001**, *342*, 265−271.
(22) Chen, J.; Liu, H.; Weimer, W. A.; Halls, M. D.; Waldeck, D. H.; Walker, G. C. *J. Am. Chem. Soc*. **2002**, *124*, 9034.
(23) Star, A.; Steuerman, D. W.; Heath, J. R.; Stoddart, J. F. *Angew. Chem., Int. Ed.* **2002**, *41*, 2508.
(24) Shvartzman-Cohen, R.; Nativ-Roth, E.; Levi-Kalisman, Y.; Yrushalmi-Rozen, R. *Langmuir* **2004**, *20*, 6085−6088.
(25) Bandyopadhyaya, R.; Nativ-Roth, E.; Regev, O.; Yerushalmi- Rozen, R. *Nano Lett.* **2002**, *2*, 25−28.
(26) Strano, M. S.; Moore, V. C.; Miller, M. K.; Allen, M. J.; Haroz, E. H.; Kittrell, C.; Huage, R. H.; Smalley R. E. *J. Nanosci. Nanotechnol*. **2003**, *3*, 81−85.
(27) Girifalco, L. A.; Hodak, M.; Lee, R. S. *Phys. Rev. B* **2000**, *62*, 13104−13110.
(28) Szleifer I.; Carignano, M. A. *Adv. Chem. Phys*. **1996**, *94*, 165−260.
(29) Szleifer I.; Carignano, M. A. *Macromol. Rapid Commun.* **2000**, *21*, 423−448.

Nanoledge France (SWNTRW,www.nanoledge.com), and SWNTK1M was purchased from NanoCarbLab (MedChemLabs division) Russia (www.nanocarblab.com).

The samples contain 40−80 wt % SWNTs, with a typical diameter of 1.3−1.4 nm and length of hundreds of nanometers to tenths of microns. Reported impurities consist of graphite, metal catalyst, and amorphous carbon. The sample designated SWNTK1M was treated by the manufacturer: temperature treatments in air flow were used to remove amorphous carbon and graphite, and acid treatments were used to remove metal particles.

Carbon fibers (Pyrograf III grade PR-24-PS (D 364) prepared via chemical vapor deposition are 30−100 μm long, with a diameter of 60−150 nm and surface area of 50−60 m^2/g, and fullerenes (Buckminsterfullerene 99.5%, Aldrich 37, 964-6, typical diameter 15 nm) were used as received.

Gum Arabic (Aldrich, Acacia 26,077-0) is a highly branched arabinogalactan polysaccharide. Millipore water (resistance of 18.2 MΩ cm) was used. Pluronic triblock: B−A−B triblock copolymer (poly(ethylene oxide)$_{100}$−*b*-poly(propylene oxide)$_{65}$−*b*-poly(ethylene oxide)$_{100}$, PEO−PPO−PEO, F127, of molecular weight 12 600 g/mol were used. The sample was obtained as a gift from BASF AG Germany. A−B diblock copolymer, poly(styrene-b−*tert*-butyl acrylate), PS−*t*buAC, Mn polystyrene 1900 acrylate 31 900 M_w/M_n 1.49, was purchased from Polymer Source Canada (Polymer source, Canada).

Methods. Preparation: Dispersions were prepared by dissolving a polymer in a solvent(aqueous or organic) to form solutions of desired concentrations. As-prepared powder (of SWNTs, carbon fibers of fullerenes) was sonicated at very mild conditions (50 W, 43 kHz) for 15−20 min in the polymeric solution. Centrifugation (3600 rpm, 30 min, room temperature) of the sample was followed by decantation of the supernatant from above the precipitate.

SEM Analysis: Dispersions of SWNTs in GA (both the supernatant and precipitate) were air-dried. The dried materials, as well as the as-received SWNT powders, were ground in a mortar (each one separately), and the powder was fixed to an aluminum stub using double-sided carbon tape and sputter-coated with 1.2 nm thick chromium using an Emitech k575x sputter machine. The samples were examined with an FEI FEG ESEM XL30.

Energy dispersive spectrometry (EDS) analysis: Dried samples (prepared as described above) were sputter-coated with gold and examined by FEI Quanta 200 SEM equipped with a Si/Li detector at 25 kV.

Transmission electron microscopy (TEM) analysis: The dispersed SWNTs were characterized via direct imaging of the aqueous dispersions using cryo-TEM.[30] Dried polymer-coated powders were imaged by TEM.

Samples for TEM imaging were prepared by placing a droplet of the dispersion on a lacey TEM grid (300 mesh Cu: Ted Pella) and allowing the water to evaporate. Imaging was carried out using JEOL 2010 (equipped with Gatan 794 CCD camera) operated at 200 kV.

Samples for cryo-TEM were prepared by placing a droplet on a grid, followed by blotting the excess liquid. Then, the specimen was vitrified by a rapid plunging into liquid ethane precooled with liquid nitrogen, in a controlled environment vitrification system. The vitrified samples were transferred to a cryospecimen holder (Gatan model 626) and examined at −178 °C in low-dose mode. Imaging was carried out using FEI Tecnai 12 G^2 (equipped with Gatan 794 CCD camera) operated at 120 kV.

Theoretical Approach

In this study we apply an extension of the single-chain mean-field theory to study theoretically the role of the polymers in stabilizing dispersions of individual SWNTs and colloidal particles. The predictions from this theory, for the structure and thermodynamic properties of polymers end-tethered to planar, spherical, and cylindrical geometries, have been shown to be in excellent quantitative agreement as compared to experimental observations[31,32] and full-scale computer simulations.[33]

In this approach each polymer molecule is considered in an exact way (within the chosen molecular model), while the intermolecular interactions are considered within a mean-field approximation. Thus, for each polymer conformation the intramolecular and polymer−SWNT interaction are exactly accounted for. The mean-field interactions are determined by the average properties of the polymer chain, in a self-consistent manner. The theory is explained in detail in refs 28 and 29, yet we stress here that we explicitly consider the inhomogeneities of the system in two dimensions and, thus, can calculate SWNT−SWNT interactions and the molecular organization and deformation of the tethered polymers as a function of the distance between SWNTs with the appropriate geometric description.

In Figure 1 we describe the system: it consists of two parallel, infinite SWNTs, of diameter 1 nm each, that are at a distance D from each other. Each SWNT is decorated by N_l end-tethered chains, e.g., poly(ethylene oxide) (PEO). We assume here that chain tethering is irreversible (either due to chemical end-grafting or due to strong adsorption of one of the blocks). The number of polymer chains per unit length is σ_{li}, with $i = 1$ and 2 for nanotube 1 and 2, respectively. The two SWNTs are embedded in a low molecular solvent, e.g., water, of molecular volume ν_w, a good solvent (athermal) environment for PEO. Note the overcrowding of polymers in the intertube region.

This system is geometrically inhomogeneous in the x,y plane. Thus, we write the Helmholtz free energy density, per unit length of nanotube, of the model polymer−solvent−nanotubes system, when the distance between nanotubes is D, by

$$\frac{\beta F(D)}{L} = \sigma_{l1}\sum_{\alpha_1} P(\alpha_1;D)\ln P(\alpha_1;D) + \sigma_{l2}\sum_{\alpha_2} P(\alpha_2;D)\ln P(\alpha_2;D) + \int\int \phi_s(x,y)\ln \phi_s(x,y)\,dx\,dy \quad (1)$$

where $P(\alpha_i;D)$ represents the probability to find a polymer grafted on nanotube i in conformation α_i, when there is another nanotube at distance D. $\phi_s(x,y)$ is the volume fraction of solvent at x,y. The first two terms in the free energy expression represent the conformational entropy of the polymer chains, and the last term is the translational (mixing) entropy of the solvent molecules. There are no attractive interactions because we assume that the solvent is good. Furthermore, the repulsive interactions are separated into intramolecular, polymer−SWNT, and intermolecular. The intramolecular and polymer−SWNT contributions are calculated exactly. The set of conformations considered, α_i, only includes self-avoiding chains that are tethered to the surface of the tube and do not have any segment in the inner region of the SWNT. The intermolecular (hard-core) repulsions are included through local packing constraints,

(30) Talmon, Y. In *Cryo techniques in biological electron microscopy*; Steinbrecht, R. A., Zierold, K., Eds.; Springer-Verlag: Berlin, 1987.

(31) (a) Szleifer, I. *Curr. Opin. Colloid. Interface Sci.* **1996**, *1*, 416−423. (b) Faure, M. C.; Bassereau, P.; Carignano, M. A.; Szleifer, I.; Gallot, Y.; Andelman, D. *Eur. Phys. J. B* **1998**, *3*, 365−375.

(32) Carignano M. A.; Szleifer, I. *Macromolecules* **1995**, *28*, 3197−3204.

(33) Carignano M. A.; Szleifer, I. *J. Chem. Phys.* **1995**, *102*, 8662−8669.

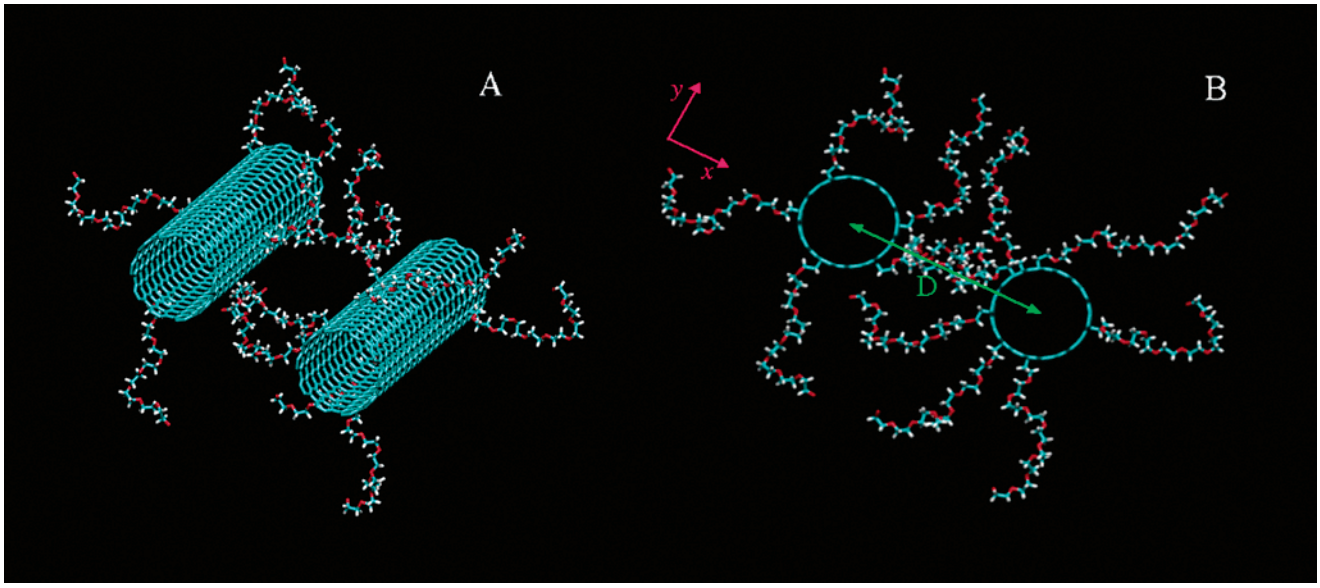

Figure 1. Different views of PEO decorated SWNTs, in good solvent conditions for the PEO chains. (A) A three-dimensional perspective and (B) a projection in the plane perpendicular to the nanotubes' axes. The coordinate system used is that used in the theoretical description, and D is the distance between the SWNT centers.

i.e., incompressibility. Namely, at each region defined between x, $x + \mathrm{d}x$ and y, $y + \mathrm{d}y$, the volume available is occupied by polymer segments or by solvent molecules

$$\langle\phi_p(x,y)\rangle + \phi_s(x,y) = 1 \tag{2}$$

for all space but the region inside the nanotubes. The polymer volume fraction contains the sum of contributions from the polymers tethered to SWNT 1 and 2 and is explicitly given by

$$\langle\phi_p(x,y)\rangle = \sigma_{l1}\sum_{\alpha_1}P(\alpha_1;D)\ \upsilon_1(x,y;\alpha_1) + \sigma_{l2}\sum_{\alpha_2}P(\alpha_2;D)\ \upsilon_2(x,y;\alpha_2) \tag{3}$$

where the first (second) term corresponds to the average volume fraction of the polymers tethered to SWNT 1 (2). $\upsilon_i(x,y;\alpha_i)\ \mathrm{d}x\ \mathrm{d}y$ is the volume that a polymer molecule in conformation α_i tethered to nanotube i occupies in the region x,y.

The next step is to find the probability of the polymer conformations and the solvent density profile. To this end we minimized the free energy, eq 1, subject to the packing constraints, eq 2 with the use of eq 3. The minimization is carried out with the help of Lagrange multipliers, $\beta\pi(x,y)$, to yield

$$P(\alpha_i;D) = \frac{1}{q_i(D)}\exp[-\beta\int\int\pi(x,y)\upsilon_i(x,y;\alpha_i)\ \mathrm{d}x\ \mathrm{d}y] \tag{4}$$

for the probability of chain i in conformation α_i, with $q_i(D)$ being the partition function that ensures the normalization of the probability at each distance D.

The solvent density profile is given by

$$\phi_s(x,y) = \exp[-\beta\pi(x,y)\upsilon_w] \tag{5}$$

indicating that the Lagrange multipliers are the osmotic pressures at x,y and ensuring that the solvent chemical potential is constant throughout; see refs 28 and 29.

Introducing the explicit expressions for the probabilities, eq 4, and the solvent density profile, eq 5, into the free energy expression, eq 1, we obtain

$$\frac{\beta F(D)}{L} = -\sigma_{l_1}\ln q_1(D) - \sigma_{l_2}\ln q_2(D) - \int\int\pi(x,y)\ \mathrm{d}x\ \mathrm{d}y \tag{6}$$

with the partition function of polymer i given by

$$q_i(D) = \sum_{\alpha_i}\exp[-\beta\int\int\pi(x,y)\ \upsilon_i(x,y;\alpha_i)\ \mathrm{d}x\ \mathrm{d}y] \tag{7}$$

The last step is to find the Lagrange multipliers. To this end, the explicit expressions for the probability of the chain molecules, eq 4, and the solvent density, eq 5, are introduced into the packing constraints, eq 2 with eq 3. The input necessary to solve the equations include (i) the grafted polymer density on each nanotube, σ_{li}; (ii) The grafted polymers chain conformations, from which the quantities $\upsilon_i(x,y;\alpha_i)\ \mathrm{d}x\ \mathrm{d}y$ are obtained; and (iii) the distance between SWNTs, D.

In practice we discretize the x,y plane into squares of side length δ, thus converting the integral equations into a set of coupled nonlinear equations. For example, the probability of the polymer chains grafted onto SWNT 1 becomes

$$P(\alpha_i;D) = \frac{1}{q_1(D)}\exp\Big[-\sum_k\sum_l\pi'(k,l)\ n_1(k,l;\alpha_1)\Big] \tag{8}$$

where the dimensionless osmotic pressure has been defined by $\pi'(k,l) = \int_{(k-1)\delta}^{k\delta}\int_{(l-1)\delta}^{l\delta}\beta\pi(x,y)\ \mathrm{d}x\ \mathrm{d}y$ and $n_1(k,l;\alpha_1)$ is the number of polymer segments that the polymer in conformation α_1 has in the region k,l.

To model the chains we make use of the rotational isomeric state model previously applied by us[31] to model PEO chains. We allow for three isoenergetic states per bond. The bond length, representing the size of an ethylene oxide monomer, is taken to be 0.3 nm. For each chain length, the conformations are generated once, and that set of self-avoiding chains that are also avoided from the inner region of the SWNTs is used in all the

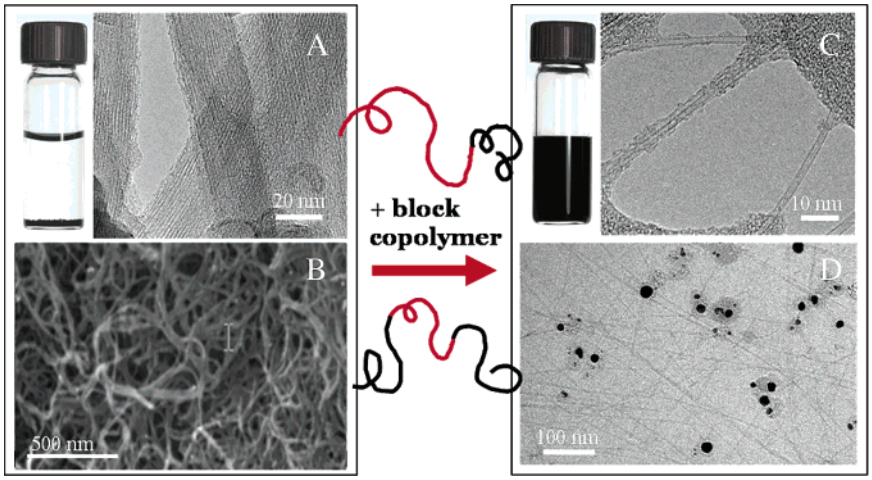

Figure 2. As-prepared SWNTs are highly bundled as observed via (A) TEM and (B) SEM imaging. Sonication leads to temporary exfoliation and deagglomeration of SWNT bundles.[26] In the absence of a dispersing agent, unmodified SWNTs reagglomerate regaining their stable bundled state. In the presence of block copolymers, under specific solvent conditions,[34] SWNTs form stable dispersions of individual tubes, as indicated by HRTEM (C) and cryo-TEM (D) of the dispersions.[35]

calculations presented below. We use a set of 10^5 independent bond sequences, generated by simple sampling. Each bond sequence enters into the calculations at 12 different angles to account isotropically for all the possible orientations with respect to the SWNTs. Indeed we find that for a single SWNT, the distribution of polymer segments is perfectly isotropic in the x,y plane. We have checked that increasing the number of conformations does not change the results presented.

In the calculations we use $\delta = 0.55$ nm and solve a number of nonlinear equations that depend on the chain length: we always reach a large enough intertube distance where the chains tethered to SWNT 1 do not see the chains from SWNT 2. For example, for $n = 50$ the maximal distance between nanotubes is 20δ. Therefore, we solve a system of 2400 nonlinear coupled equations, i.e, 60 in the x direction and 40 in the y direction; see Figure 1. However from symmetry considerations (Figure 1) practically only half of the equations are independent. Thus, for the largest distance we solve 1200 nonlinear coupled equations each with some 10^6 terms (one per chain conformation and angle) via standard numerical methods, for the shortest distance, $D = 2R$, the number of equations reduces to 840 for this chain length.

Results and Discussion

Recently we found that a large variety of synthetic block copolymers[24] and the natural polysaccharide GA[25] efficiently disperse SWNTs in organic as well as in aqueous solutions, up to high concentrations of individual SWNTs. Moreover, the dispersions could be dried and redispersed, preserving the deagglomerated state of the SWNTs. X-ray scattering and TEM provide clear evidence for the individual-tube nature of the dispersed moieties. In Figure 2 we summarize our previous findings (detailed in refs 24 and 25).

In the following we present a detailed theoretical description of the system and examine quantitatively the effect of polymers on the inter-SWNT potential.

In Figure 3 we present the calculated intertube potential for two parallel SWNTs as a function of the intertube distance. The intermolecular interactions between SWNTs are derived using the model by Girifalco et al.[27] A large attractive interaction at short distances is observed, with a minimum of 35 K_bT/nm. The

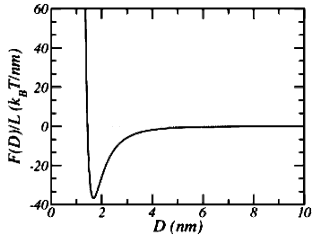

Figure 3. Potential of interaction between two parallel SWNTs as a function of the distance between them, as calculated by Girifalco et al.[27] Note the very deep attractive well when the SWNTs are at contact.

interaction is short ranged and decreases to below K_bT within 5 nm. This is an interesting aspect of SWNT intermolecular behavior, which results from the fact that two of the dimensions of the particles are nanometric.

In the next stage we calculate the intertube potential for SWNTs decorated by (end-tethered)[35] PEO chains of 50, 100, and 150 segments (these chain lengths are relevant to the experimental data), at three different values of surface coverage. Note that in the model presented here we assume that the two polymer blocks play a very different role due to the selectivity of the solvent: the block for which the solvent acts as a poor solvent adsorbs to the SWNTs and anchors the other block, the tail, which dangles into the solvent and is swollen by it (Figure 1). In Figure 4 we present the polymer-induced repulsion among decorated SWNTs, in good solvent conditions for the polymer tails.

Indeed, we observe that the range and strength of the repulsion increase with increasing the length of the grafted chains. The effect of surface coverage is somewhat different: while the strength of the repulsion increases with surface coverage, the range of the interaction is only mildly changed.

(34) The quality of the solvent is characterized by the balance of inter- vs intramolecular interactions. In the mean-field framework the Flory interaction parameter $\chi = \chi_{MS} - {}^1/_2(\chi_{MM} + \chi_{SS})$ is used to describe the balance (where χ_{MM} is the monomer interaction, χ_{MS} is the monomer−solvent interaction, and χ_{SS} is the solvent−solvent interaction). Good solvents are those characterized by low χ, while poor (bad) solvents have a high χ. A detailed description of the approach and a list of good and poor solvents for different polymers can be found in the handbook by Van Krevelen, D. W. *Properties of Polymers*, 3rd ed.; Elesvier: Amsterdam, 1990.

(35) In Figure 2 we present electron microscopy images of as-prepared SWNTs (A) SWNTK1M and (B) SWNTAP and of dispersions of SWNTAP (C) 1 wt % in a solution of 1 wt % of PS-*t*buAC in ethanol and (D) 2.5 wt % of SWNTAP in 1 wt % PE10500 in water. Additional details of the polymers and the dispersions are given in ref 25.

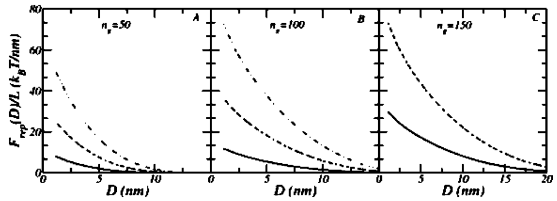

Figure 4. Repulsive component of the interaction between parallel SWNTs with tethered polymers, as a function of the distance between the nanotubes. The steric repulsion due to the tethered polymers is calculated using eq 6. The three graphs correspond to different polymer chain lengths as denoted in the figures. For each polymer molecular weight, the numbers of polymer grafted per unit length are (i) $\sigma_l = 2$ nm^{-1} (full line); (ii) $\sigma_l = 4$ nm^{-1} (dashed line); and (iii) $\sigma_l = 6$ nm^{-1} (dot−dashed line).

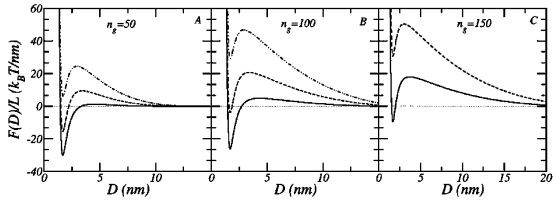

Figure 5. Total interaction energy between parallel SWNTs with tethered polymers. The total interaction is obtained by adding the attractive component, as given in Figure 3, and the repulsive component, Figure 4. The different polymer chain lengths are denoted in the figures, and the lines are as those in Figure 4.

Note the different distance scales for the three polymer chain lengths. For the longest polymer we do not show the highest surface coverage, since the other two already present a very large repulsive interaction.

Examination of the range of SWNT−SWNT attractions presented in Figure 3 and that of the repulsions in Figure 4 suggests that for all chain lengths and surface coverage the range of the repulsive, interpolymer interactions is longer than the range of the intertube attraction.

The overall interaction profile for polymer coated SWNT is presented in Figure 5.

The results of Figure 5, and related calculations, can be used to determine the minimal polymer coverage necessary to stabilize the SWNTs. However, since the position of the maxima changes, one can construct a lower bound limit. Consider for example that in all cases shown the maximum is found around a distance of 3 nm or larger, Figure 5. Then, we take the bound to be 3 nm and determine for each polymer molecular weight the number of polymers per unit length necessary to create a barrier of at least 5kT/nm. We call this quantity σ_l^*. Since the attraction at 3 nm is, from Figure 2, −6kT/nm, we are looking for a repulsive interaction at 3 nm of 11kT/nm. We find the minimal values to be $\sigma_l^* = 3.4$ nm^{-1}, $\sigma_l^* = 2.4$ nm^{-1} and $\sigma_l^* = 1.0$ nm^{-1} for polymers with 50, 100, and 150 segments, respectively. This calculation can in principle be repeated as a function of the CNT diameter and thus obtain the optimal surface modification with polymer chain length.

For the two shortest chain lengths shown above, polymers tethered at low surface coverage present a rather weak repulsion. In all other cases the effective potential exhibits a large barrier (local maxima). Namely, a repulsive energy that is large enough to prevent the SWNTs from reaching the attractive part of the potential at small intertube separations is set up.

While the repulsive part of the effective potential can be modified via the polymer chain length and surface coverage, the short range and steepness of the attractive component of the interaction (Figure 3) imply that the intertube distances at the maximum and minimal free energy are independent of polymer surface coverage and chain length. Therefore, while it is possible to tune the range of the repulsive tail of the potential and the strength of the maximum and minimum, the position of the latter two is fixed.

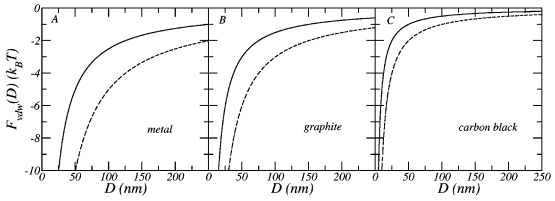

Figure 6. vdW free energy between two spherical particles as a function of interparticle separation (D). The relation was calculated using the expression $W = -A/6DR_1R_2/(R_1 + R_2)$ (ref 4, p 177) for particles of a diameter of 50 nm (full line) and 100 nm (dashed line) of (A) metal, characterized by $A = 5 \times 10^{-19}$ J; (B) graphite, $A = 3 \times 10^{-19}$ J; and (C) carbon black, $A = 1 \times 10^{-19}$ J.

The results presented in Figure 5 suggest that, in the case of SWNTs, the short range of the attraction gives rise to a simple, generic scenario where steric repulsion among polymers may lead to stabilization of SWNT dispersions. Clearly, the first step in this scenario is to separate the SWNTs (for example, via mild sonication which does not damage the tubes),[24−26] and that enables the tethering of the polymers. Once the polymers are attached to the surface, they present a steric barrier under almost all relevant conditions and thus effectively maintain the nanotubes separated in solutions.

The behavior presented in Figure 5 is fundamental in classical colloidal stabilization. Yet, one point deserves special attention: Unlike classical colloids, SWNTs are molecular objects, with two dimensions in the nanometric range. Thus, the attractive part of the potential is short ranged, and short polymers are able to stabilize the individual tubes (Figure 5). Figure 6 shows the vdW potential between submicron particles. The interaction is significant even at distances larger than the particle's radius showing the colloidal character of the interactions. This is due to the additivity of the vdW interactions as manifested in the Hamaker constant.

To estimate the effect of end-tethered polymers on colloidal particles, we estimated the interaction between parallel planar surfaces decorated by grafted polymers in good solvent conditions. This system provides an upper bound for the repulsive interaction induced by tethered polymers and serves to examine the effect of the strongest possible repulsions. The interactions between grafted polymer layers on planar surface are well described by the Alexander−de-Gennes theory.[37] According to the model, the thickness of the polymer layer, L, is given by $L = cl\sigma^{1/3}n$, where c is a constant of order unity and l is the segment length. The thickness of the layer determines the range of the interaction, and this in turn determines the ability of the polymer layer to prevent flocculation (and stabilize the dispersion). Considering the longest chains with $n = 150$ and $l = 0.3$ nm, we find that the repulsion exceeds K_bT at $D < 45$ nm. Comparison to the potentials presented in Figure 6 suggests that this distance is shorter than the range of the attractive interactions (apart from carbon black, to be discussed below), and

(36) For block copolymers an equivalent assumption is that a triblock copolymer, B−A−B, is tethered to the surface via the A block.
(37) Alexander, S. *J. Phys. (Paris)* **1977**, *38*, 977.

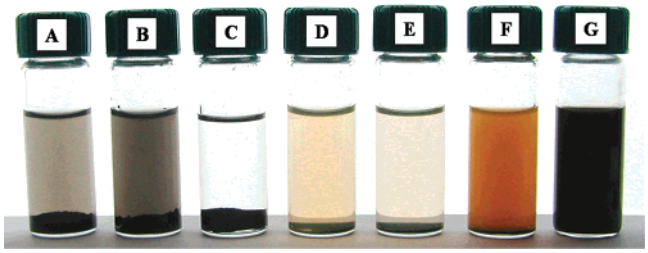

Figure 7. Dispersions of different carbonaceous species following sonication in solutions of 0.5 wt % of carbon fibers in (A) aqueous solution of 5 wt % GA, (B) aqueous solution of 5 wt % F127, and (C) 5 wt % PS-*t*buAC in ethanol. 1.5 wt % of fullerenes in (D) aqueous solution of 5 wt % GA, (E) aqueous solution of 5 wt % F127, and (F) 5 wt % PS-tbuAC in ethanol. (G) 1 wt % of SWNTAP in aqueous solution of 5 wt % F127.

therefore we expect the polymer layer to be ineffective in stabilization of these particles.

To test these ideas, we performed the following set of experiments: Following the procedure described in the Experimental Section, we sonicated carbon fibers and fullerenes in aqueous solutions of GA and F127 and in ethanol solution of PS−*t*buAC at concentrations in the range of 1−10 wt %. An image of vials containing dispersions of the different species is shown in Figure 7.

We observe that carbon fibers (Figure 7A−C) and fullerenes (Figure 7D−F) were not dispersed in the polymer solutions unlike SWNTs (Figure 2 and previous work) but rather coagulated and precipitated, unlike SWNTs under similar conditions (Figure 7G). These observations indicate that the different polymers do not disperse carbon fibers and fullerenes, while they efficiently disperse SWNTs, in accordance with the model presented above. Similar results were obtained for submicron graphite flakes (not shown).

To further test the possibility of using the dimensional selectivity for purification of SWNT−colloidal mixtures, we examined the behavior of as-prepared powders of SWNTs that is known to contain a high percentage of carbonaceous impurities (fullerenes, amorphous carbon, carbon coated metal particles).

A powder containing 40−60 wt % of SWNTs along with carbonaceous impurities and metal catalyst (SWNTAP, SWNTRW) was sonicated in polymeric solutions (GA and Pluronic F127). Dispersions were prepared by sonicating at low power (50 W for 30 min) a powder of as-prepared SWNTs (at concentrations between 0.2 wt % and 10 wt %) in polymer solutions (0.5 wt % to 15 wt %, polymer weight per water weight). A black, homogeneous inklike suspension was obtained, along with a black precipitate. Centrifugation (3600 rpm, 30 min, room temperature) of the sample was followed by decantation of the supernatant from above the precipitate.

Both supernatant and precipitate were imaged by electron microscopy, their composition analyzed via EDS. In Figure 8 we present SEM images of SWNTAP.

The raw powder (Figure 8A) is characterized by the presence of fiberlike entities together with many nontubuline structures. The typical diameter of the fibers is in the range of few tens of nanometers, as expected for ropes where each is composed of many tubes. In Figure 8B we present an image of a powder obtained by drying the supernatant phase of SWNTAP dispersed in GA solution. The sample seems to contain much less of the nontubuline moieties than the raw powder (Figure 8B). The precipitate (Figure 8C) is highly enriched by non-SWNT structures.

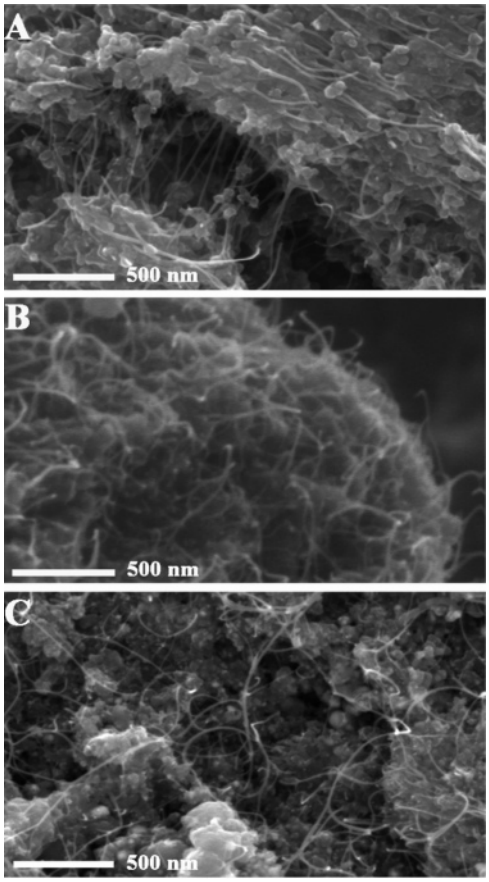

Figure 8. SEM micrographs of (A) as-prepared SWNTAP powder, (B) a dried supernatant phase of a 1 wt % SWNTAP and 1 wt % GA (termed 1:1 wt %) dispersion, and (C) the dried precipitate of the same dispersion. The samples were examined at 10 kV (A) and at 5 kV (B, C).

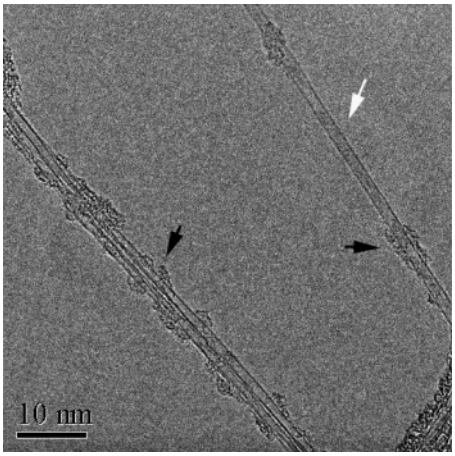

Figure 9. TEM image of redispersed SWNTAP (1:2 wt % SWNTAP to GA in aqueous media). The sample was prepared by drying the supernatant phase and redispersing it in a small volume of water. The white arrow points at an individual tube, and the black arrows indicate carbonaceous species on the tubes.

TEM imaging of the supernatant phase reveals the presence of individual tubes and small bundles containing 2−3 tubes (Figure 9, white arrow). Carbonaceous species that have probably grown onto the tubes during the synthesis[18] are also shown (Figure 9, black arrows).

Table 1. Metal Atom % in Polymer-Treated SWNT Samples (Polymer/SWNT 1:1 wt %) as Measured via EDS

sample	as-prepared	dried supernatant phase	dried precipitate
(a) SWNTAP in GA	5 ± 1.4	2 ± 0.7	7.5 ± 0.8
(b) SWNTRW in GA	2 ± 1.1	0.6 ± 0.2	2 ± 0.8
(c) SWNTAP in F127	5.8 ± 1.4	1.4 ± 0.7	4.7 ± 0.8

The relative metal content of the supernatant phase and the precipitate (obtained by dispersing SWNTAP or SWNTRW at 1:1 weight ratio in aqueous solutions of the polymers) were measured via EDS (Table 1).

The values presented in Table 1 indicate that the relative concentration of metals in the precipitate is significantly higher than that in the supernatant. Additional experimental evidence for the compositional difference between the two phases as observed by thermogravimetric analysis can be found in the Supporting Information.

In a different series of experiments, we collected the precipitate, dried the powder, and redispersed it in water. We observed that though some of the precipitate floated in the liquid, most of it could not be redispersed. This observation indicates that simple partitioning of the carbon soot between the two phases cannot be the origin of the observed effect, but rather the precipitate is composed of nondispersible moieties, suggesting that the interaction between the polymers and SWNTs is selective.

The observed selectivity is an important consequence of the dependence of the intertube potential on the dimensions of the colloidal particles. Using relatively short polymeric chains for steric stabilization, we find that while polymer-decorated SWNTs experience large enough repulsion that results in the formation of stable dispersions, carbonaceous particles (of similar density) but of submicron diameter will coagulate and flocculate.

Similar observations were reported for other polymers and solvents: Yudasaka et al. reported selective dispersion of SWNTs (prepared via laser ablation) by poly(methyl methacrylate) (PMMA) in monochlorobenzene solutions.[38] A. B. Dalton et al. reported the selective dispersion of SWNTs (prepared via arc discharge) in toluene solutions of poly(*p*-phenylenevinylene-*co*-2,5-diotoxy-*m*-phenylenevinylene) (PmPV).[39] We believe that these observations may be rationalized by the model presented here.

The last point relates to carbon black. The calculations presented in Figure 6 suggest that for carbon black particles with a radius of 50 and 100 nm the range and depth of the attractive interaction are much reduced. This is a direct manifestation of the lower values of the effective Hamaker constant due to the relatively low particle density (high porosity). Indeed previous studies[40] indicate that Pluronic polymers disperse well carbon black in aqueous solutions, and as was described in the Introduction, dispersion of carbon black in GA solutions is one of the earliest demonstrations of steric stabilization.

Conclusions

We previously found experimentally that it is possible to stabilize dispersed individual SWNTs in aqueous and organic solvents using relatively short tethered polymers in selective solvents. The theory presented here suggests that this behavior originates from the combination of the short range and steepness of the attractive component of the SWNT−SWNT potential, together with the range of polymer-induced repulsion. We also observed that for different colloidal particles the range of the attractive interactions is determined by the number of microscopic vs mesoscopic dimensions. For SWNTs where two of the dimensions are nanoscopic and one is mesoscopic, the attractive potential is relatively short ranged, albeit very steep. Therefore, even short polymer chains can produce a long enough repulsive potential that results in large enough repulsive barriers to stabilize a dispersion of the individual tubes. In the case of submicron colloidal particles the attractive vdW potential is proportional to the product of the Hamaker constant and the particle radius. Typically, this product results in a significant attraction at distances larger than the size of the particles. Therefore, the polymer chain length and surface coverage necessary for inducing steric repulsion in colloidal dispersions are much higher than those required for dispersion of SWNTs.

The effect described above suggests that polymers offer a generic pathway for stabilization of SWNT dispersions, and a proper choice of the polymer molecular weight may result in dimensional selectivity enabling purification of SWNTs from mixtures of non-nanometric objects.

Acknowledgment. This research was supported by the Israel Science Foundation, the Center of Excellence Program (Grant No. 8003) and at Purdue by the National Science Foundation Grant CTS-0338377 and the Indiana 21st Century Research and Technology Fund. The authors thank Dr. Marcelo Carignano for insightful discussions and for the preparation of Figure 1.

Supporting Information Available: TGA behavior of the supernatant phase and the precipitate was studied. Mass change was measured as a function of the temperature during a heating procedure from 40 °C to 1000 °C at a rate of 10 °C min^{-1} under a constant flow of air (200 mL min^{-1}). The amount of the metal catalyst in each phase is revealed by the weight remain without being burned up to 1000 °C. TGA traces of the supernatant and the precipitate phases indicate that the relative concentration of metals in the precipitate is significantly higher than in the supernatant.

JA046377C

(38) Yudaska, M.; Zhang, M.; Jabs, C.; Ijima, S. *Appl. Phys. A* **2000**, *71*, 449−451.
(39) Dalton, A. B.; Blau, W. J.; Chambers, G.; Coleman, J. N.; Henderson, K.; Lefrant, S.; McCarthy, B.; Stephan, C.; Byrne, H. J. *Synth. Met.* **2001**, *121*, 1217−1218.
(40) Lin, Y.; Alexandridis, P. *J. Phys. Chem. B* **2002**, *106*, 10834−10844.